

# Off equilibrium dynamics in disordered quantum spin chain

Stéphane Abriet and Dragi Karevski

Laboratoire de Physique des Matériaux, UMR CNRS No. 7556, Université Henri Poincaré (Nancy 1), B.P. 239, F-54506 Vandœuvre lès Nancy cedex, France

July 1, 2002

**Abstract.** We study the non-equilibrium time evolution of the average transverse magnetisation and end-to-end correlation functions of the random Ising quantum chain. Starting with fully magnetised states, either in the  $x$  or  $z$  direction, we compute numerically the average quantities. They show similar behaviour to the homogeneous chain, that is an algebraic decay in time toward a stationary state. During the time evolution, the spatial correlations, measured from one end to the other of the chain, are building up and finally at long time they reach a size-dependent constant depending on the distance from criticality. Analytical arguments are given which support the numerical results.

**PACS.** 75.40.Gb Dynamic properties (dynamic susceptibility, spin waves, spin diffusion, dynamic scaling, etc.)

05.70.Ln Non-equilibrium and irreversible thermodynamics

05.30-d Quantum statistical mechanics

## 1 Introduction

Non-equilibrium properties of quantum spin chains at very low or even zero temperature have been the subject of several investigations through decades. Some precursor studies were done by Niemeijer [1] and Tjion [2] at the end of the sixties. They have shown that the relaxation is algebraic instead of exponential as predicted by Terwiel and Mazur using a weak coupling limit [3]. More recently, several authors have considered the relaxation of inhomogeneously magnetised initial states and obtained analytical results for various classes of free fermionic spin chains [4,5,6,7,8]. It was pointed out in ref. [7] that at some special wave vectors, characterizing the inhomogeneity of the initial state, a slowing down of the relaxation can occur for free fermionic models that have a gapped excitation spectrum. In the context of aging phenomena, two-time non-equilibrium functions were considered in ref. [6,9] for the Ising and XX quantum chains. Aging occurs for intermediate times in such systems. All these out of equilibrium studies were done for systems without any disorder although alternating and dimerized models were also considered previously [7]. In this work we study the influence of random spin couplings on the non-equilibrium relaxation properties. For that purpose we consider the paradigmatic random Ising quantum chain.

The paper is organized as follows: in section 2 we present the random Ising quantum chain and discuss some of its main equilibrium properties. After the canonical diagonalization, we express the time-dependent operators we are interested in. In the next section, we first give the general expressions for the non-equilibrium quantities we

are considering, namely transverse magnetisation and end-to-end correlation functions for two different initial states and give the numerical results and analytical analysis of this quantities. The last section summarizes and discusses our results.

## 2 Random Ising quantum chain

The Hamiltonian of the random Ising quantum chain is given by

$$H = - \sum_k J_k \sigma_k^x \sigma_{k+1}^x - \sum_k h_k \sigma_k^z \quad (1)$$

where the  $\sigma$ s are the Pauli matrices and  $J_k$  and  $h_k$  are random independently distributed couplings and transverse fields. The system possesses a quantum phase transition at zero temperature controlled by the parameter

$$\delta = [\ln h] - [\ln J], \quad (2)$$

where  $[\cdot]$  means an average over the disorder distribution. The quantum control parameter  $\delta$  separates the paramagnetic phase ( $\delta > 0$ ) from the ferromagnetic one ( $\delta < 0$ ). Exactly at  $\delta = 0$  the system is at the critical point. This system has been studied intensively by numerical and analytical means. In particular, using a RG procedure initially introduced by Ma, Dasgupta and Hu [10], Fisher has obtained asymptotically exact results (confirmed by numerical works) on the static properties and equal time correlations in the vicinity of the critical point [11]. In

addition to Fisher's results, new numerical and analytical results have been obtained by various methods and mappings away from the critical point [12,13,14,15], in the so called Griffiths phase [16,17]. In particular, the behaviour of the singular quantities in the Griffiths phase are all characterized by a single dynamic exponent  $z(\delta)$ , which is continuously varying with the control parameter  $\delta$  [14,15]. More recently, Iglói has extended the exact RG treatment of Fisher into the Griffiths phase on both sides of the critical point [18,19].

The Hamiltonian (1), with free boundary conditions and  $L$  sites, is readily diagonalized after a Jordan-Wigner mapping [20]

$$\begin{aligned} A_n &= \prod_{i=1}^{n-1} (-\sigma_i^z) \sigma_n^x \\ B_n &= i \prod_{i=1}^{n-1} (-\sigma_i^z) \sigma_n^y \end{aligned} \quad (3)$$

and a canonical transformation in terms of Fermi operators  $\eta$  and  $\eta^+$  [21]:

$$H = \sum_q \epsilon_q \eta_q^+ \eta_q + E_0 \quad (4)$$

where the excitation energies  $\epsilon_q$  are the positive solutions of the  $2L \times 2L$  eigenvalue problem

$$\mathbf{T}V_q = \epsilon_q V_q \quad (5)$$

where  $\mathbf{T}$  is the tridiagonal matrix

$$\mathbf{T} = \begin{pmatrix} 0 & h_1 & & & & \\ h_1 & 0 & J_1 & & & \\ & J_1 & 0 & h_2 & & \\ & & h_2 & 0 & \ddots & \\ & & & \ddots & \ddots & J_{L-1} \\ & & & & J_{L-1} & 0 & h_L \\ & & & & & h_L & 0 \end{pmatrix}. \quad (6)$$

The  $2L$  components eigenvectors  $V_q$  are usually split into two  $L$  components eigenvectors  $\phi_q$  and  $\psi_q$ , such that  $V_q(2k-1) = -\phi_q(k)$  and  $V_q(2k) = \psi_q(k)$ .

Stationary and time-dependent expectation values of spin operators are expressed easily in terms of the Fermi operators  $\eta_q, \eta_q^+$ . Working in direct space, it is more convenient to expand these quantities in terms of the operators  $A$  and  $B$  related to the diagonal fermions through

$$\begin{aligned} A_n &= \sum_q \phi_q(n) (\eta_q^+ + \eta_q) \\ B_n &= \sum_q \psi_q(n) (\eta_q^+ - \eta_q) . \end{aligned} \quad (7)$$

These operators satisfy the anticommuting algebra  $\{A_n, A_m\} = 2\delta_{n,m}$ ,  $\{B_n, B_m\} = -2\delta_{n,m}$  and  $\{A_n, B_m\} =$

0. From the time evolution of the diagonal Fermi operators,  $\eta_q^+(t) = e^{iHt} \eta_q^+ e^{-iHt} = \eta_q^+ e^{i\epsilon_q t}$ , one obtains the time evolution of the  $A$ s and  $B$ s:

$$A_n(t) = \sum_m \langle A_n A_m \rangle_t A_m + \langle A_n B_m \rangle_t B_m \quad (8)$$

and

$$B_n(t) = \sum_m \langle B_n A_m \rangle_t A_m + \langle B_n B_m \rangle_t B_m \quad (9)$$

where the basic contractions  $\langle \dots \rangle_t$ , proportional to the time-dependent anticommutators, are given by [9,8]

$$\langle A_n A_m \rangle_t = \sum_q \phi_q(n) \phi_q(m) \cos(\epsilon_q t) \quad (10)$$

$$\langle B_n B_m \rangle_t = \sum_q \psi_q(n) \psi_q(m) \cos(\epsilon_q t) \quad (11)$$

and

$$\langle A_n B_m \rangle_t = \langle B_m A_n \rangle_t = i \sum_q \phi_q(n) \psi_q(m) \sin(\epsilon_q t) . \quad (12)$$

For the homogeneous chain at the critical point, these contractions are simply expressed in terms of integer Bessel functions [9,8]. In the disordered situation, we evaluate them numerically.

Utilising the previous expressions, one finds for the time evolution of the  $\sigma_l^z = B_l A_l$  Pauli operator at site  $l$

$$\begin{aligned} \sigma_l^z(t) &= \sum_k (\langle B_l B_k \rangle_t \langle A_l A_k \rangle_t - \langle B_l A_k \rangle_t \langle A_l B_k \rangle_t) \sigma_k^z \\ &+ \sum_{i \neq j} (\langle B_l B_i \rangle_t \langle A_l A_j \rangle_t - \langle B_l A_j \rangle_t \langle A_l B_i \rangle_t) B_i A_j \\ &+ \sum_{i \neq j} \langle B_l A_i \rangle_t \langle A_l A_j \rangle_t A_i A_j + \sum_{i \neq j} \langle B_l B_i \rangle_t \langle A_l B_j \rangle_t B_i B_j . \end{aligned} \quad (13)$$

Contrary to the operators  $\sigma_l^z$ , the operators of the form  $B_l A_m$  are string operators in terms of the Pauli matrices. For example we have for the terms  $B_l A_m$ :

$$B_l A_{m \geq l+1} = (-1)^{l+m+1} \sigma_l^x \left( \prod_{j=l+1}^{m-1} \sigma_j^z \right) \sigma_m^x \quad (14)$$

so that in a general state it is hard to evaluate the expectations  $\langle \Psi | B_l A_m | \Psi \rangle$ . In the same way, the end-to-end correlation operator  $\sigma_1^x(t) \sigma_L^x(t)$ , which gives insight of the development of the correlations in the chain during the time evolution, is given by

$$\sigma_1^x(t) \sigma_L^x(t) = A_1(t) B_L(t) \mathcal{Q} \quad (15)$$

with

$$\mathcal{Q} = \prod_{j=1}^L (-\sigma_j^z) \quad (16)$$

the charge operator which is a conserved quantity since  $[H, \mathcal{Q}] = 0$ . Inserting the developments (8) and (9) into the expression (15), one obtains the final form of the end-to-end correlation operator.

### 3 Off equilibrium dynamics

#### 3.1 Expectation values

In what follows, we are interested in the non-equilibrium relaxation properties of the random Ising quantum chain. The time evolution of the system is governed by the Schrödinger equation and is given formally by the unitary evolution

$$|\Psi(t)\rangle = \exp(-iHt)|\Psi\rangle \quad (17)$$

since energy is conserved. The initial states we consider in this work are eigenstates of the Pauli matrices, that is either  $|x\rangle$  or  $|z\rangle$  such that  $\sigma_l^{x,z}|x, z\rangle = |x, z\rangle$ . These states are easily accessible experimentally by applying a strong magnetic field in the desired direction. The choice of such initial states is not only motivated by their physical accessibility but as well because they permit close analytical formulae for the magnetisation profile and end-to-end correlations [4,9]. Consider first the  $|z\rangle$  state. In this state, the  $\sigma^{x,y}$  operators act as flip operators and from formulae (13) and (14) the non-vanishing expectations are only those of the  $\sigma^z$  terms, such that finally we obtain

$$m_z^z(l, t) \equiv \langle z|\sigma_l^z(t)|z\rangle = \sum_k (\langle B_l B_k \rangle_t \langle A_l A_k \rangle_t - \langle B_l A_k \rangle_t \langle A_l B_k \rangle_t). \quad (18)$$

Utilising  $\mathcal{Q}|z\rangle = (-1)^L|z\rangle$ , the end-to-end correlation function in the  $z$  state for a chain of even site number is given by

$$C_L^z(t) \equiv \langle z|\sigma_1^x(t)\sigma_L^x(t)|z\rangle = \sum_k (\langle A_1 B_k \rangle_t \langle B_L A_k \rangle_t - \langle A_1 A_k \rangle_t \langle B_L B_k \rangle_t). \quad (19)$$

If the initial state is the  $|x\rangle$  state, the role of the flip operators are played by the  $\sigma^{y,z}$  operators. Then, the contributing terms into (13) are only the  $B_l A_{l+1} = \sigma_l^x \sigma_{l+1}^x$ , whose expectation value is 1 in  $|x\rangle$ . This leads to

$$m_x^z(l, t) \equiv \langle x|\sigma_l^z(t)|x\rangle = \sum_k (\langle B_l B_k \rangle_t \langle A_l A_{k+1} \rangle_t - \langle B_l A_{k+1} \rangle_t \langle A_l B_k \rangle_t). \quad (20)$$

The connected end-to-end correlation function  $C_L^x(t) \equiv \langle x|\sigma_1^x(t)\sigma_L^x(t)|x\rangle - \langle x|\sigma_1^x(t)|x\rangle \langle x|\sigma_L^x(t)|x\rangle$  is simply

$$C_L^x(t) = |\langle A_1 B_L \rangle_t|^2. \quad (21)$$

The simplicity of the formulae obtained so far is due to the locality in terms of the  $A$  and  $B$  operators of the non-vanishing expectations entering here. For other quantities, for example expectation of  $\sigma_l^x$  at a general site  $l$ , the formula is no more local and one should use Wick's theorem in order to evaluate the string operators appearing. This leads to huge determinants that are not efficiently calculable numerically, especially if one has to perform averages over disorder realizations. In this case, a direct space calculation is probably more appropriate.

#### 3.2 Results

In the numerical study, we use the following distribution for the couplings and fields:

$$\pi(J) = \begin{cases} 1 & J \in [0, 1] \\ 0 & \text{otherwise} \end{cases} \quad (22)$$

and

$$\rho(h) = \delta(h - h_o). \quad (23)$$

The critical field  $h_c$  is obtained from the vanishing of the control parameter  $\delta$ , that is  $h_c = e^{-1}$ . Average quantities

$$[Q] = \frac{1}{N} \sum_{i=1}^N Q^{(i)} \quad (24)$$

are computed using typically  $N \sim 50000$  disorder realizations for chains of size up to  $L \sim 100$ .

In figure 1 we show the time dependence of the average surface and bulk magnetisation,  $[m_z^z(1, t)]$  and  $[m_z^z(L/2, t)]$  respectively, at the critical point starting with the  $|z\rangle$  state. For long times, the non-equilibrium surface and bulk transverse magnetisations reach a size-independent constant value  $m_z^{s,b}(\infty)$ . The relaxation toward  $m_z^{s,b}(\infty)$  is clearly slower than exponential and presumably algebraic, with superimposed oscillations with period of about  $2\pi$ . This new time-scale is related to the disorder distribution properties. We have tested the robustness of those oscillations against disorder distributions. For exponential like distributions,  $P(J) = \alpha \exp(-\alpha J)$ , they have a period  $\tau$  varying linearly with the width parameter  $\alpha$ , meaning that the microscopic time scale  $\tau$  is set by the average coupling  $[J]$ , as  $\tau \sim [J]^{-1} = \alpha$ . So one expects the presence of these oscillations for every disorder distributions with a finite first momentum.

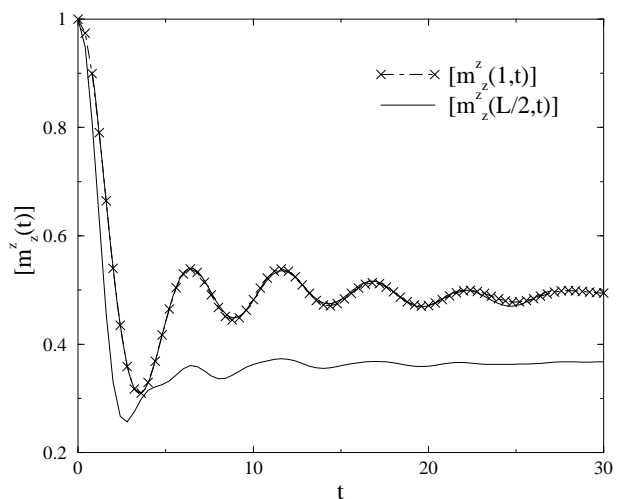


**Fig. 1.** Surface and bulk non-equilibrium average transverse magnetisation at the critical field  $h_c$  starting with the  $|z\rangle$  state. The thick line corresponds to the fit discussed in the text.

In the case of the surface magnetisation, the relaxation behaviour is very well fitted by the form  $t^{-1.15}[\cos(1.2t - 1.46) - 0.43 \cos(0.3t - 1)] + 0.5$  as shown in figure 1, which validate the power law relaxation behaviour. For the bulk magnetisation such a fit is much more hazardous since the oscillations have a more complicated structure.

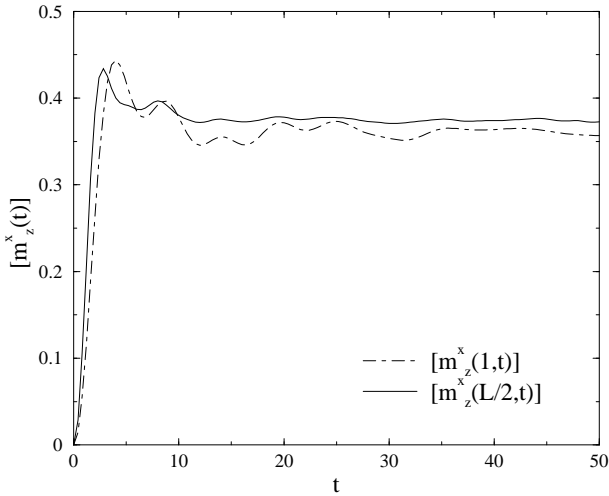


**Fig. 2.** Surface and bulk non-equilibrium average transverse magnetisation at the critical field  $h_c$  starting with the  $|x\rangle$  state.

Figure 2 shows the same quantity starting with the  $|x\rangle$  state at time  $t = 0$ . The surface and bulk non-equilibrium transverse magnetisations approach algebraically the constants  $m_x^{s,b}(\infty)$ . The features observed for the average magnetisation are very similar to the homogeneous critical case where one finds  $m_z^{z,x}(t) = 1/2 \pm J_1(4t)/4t$ , with the  $+$  ( $-$ ) sign for the  $z(x)$ -state [6,9,8]. Thus the relaxation toward  $1/2$ , is characterized by the power law  $t^{-3/2}$ .

The asymptotic values of the non-equilibrium magnetisation are depending on the value of the field  $h_o$ . We present the dependence of these quantities on the transverse field in figure 3 for increasing sizes for the disordered case. We give also, in order to compare, the exact asymptotic values for the pure case [6,9]. The behaviour of the asymptotic averaged magnetisation doesn't seem to have any singularity near the critical field contrary to the pure case. Nevertheless, finite-size effects should not be excluded too quickly in the vicinity of the critical point also the curve shown in figure 3 have almost collapsed. One may notice that as in the homogeneous situation, the asymptotic limits take the same value at the critical field for both initial states.

We turn now to the discussion of the average non-equilibrium end-to-end correlation,  $[C_L^{x,z}(t)]$ . Figure 4 show the behaviour of this quantity for various fields. Since the velocity of the excitations are finite, the end-to-end correlations are vanishing up to a threshold time  $\tau(L) \propto L$ . No signal starting from one end has yet reached the other end. For  $t > \tau(L)$ , the correlations start to build

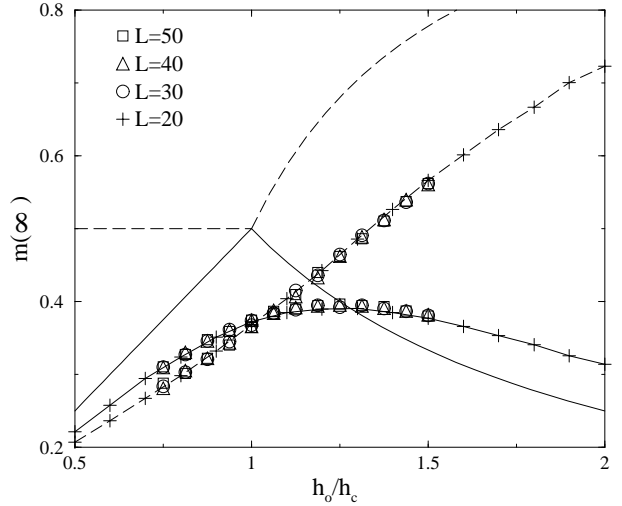


**Fig. 3.** Asymptotic values of the non-equilibrium average transverse magnetisation as functions of the distance to the critical field  $h_o/h_c$ . Lines with symbols refer to the disordered situation while thick lines to the exact pure case solutions. The solid(dashed) line corresponds to the  $|x\rangle(|z\rangle)$ .

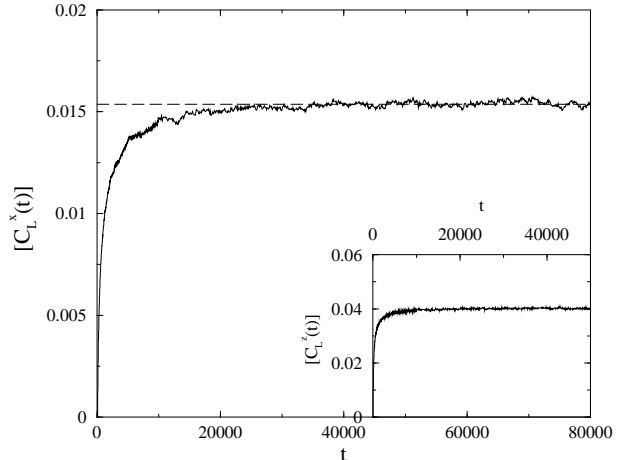


**Fig. 4.** Average end-to-end correlation functions at the critical field  $h_c$  and  $L = 20$  starting with the  $|x\rangle$  state. The dashed line is given by (27). Insert: same as before for the  $|z\rangle$  state.

up and finally for very long times they reach a finite value  $C_L^{x,z}(\infty)$  depending on  $L$ . In figure 5 we present the size dependence of the asymptotic value  $C_L^x(\infty)$  for  $h_o = h_c$ ,  $h_o > h_c$  and  $h_o < h_c$ .

The asymptotic behaviour of the end-to-end correlators can be understood as follows. To fix the ideas, consider the simple connected end-to-end correlator  $C_L^x(t) = |\langle A_1 B_L \rangle_t|^2$ . It can be split into a time-dependent quantity and a time independent part:

$$C_L^x(t) = F(L, t) + G(L), \quad (25)$$

where  $G(L) = 1/2 \sum_q \phi_q^2(1) \psi_q^2(L)$  and  $F(L, t) = \sum_{q \neq q'} \Gamma_{qq'} [\cos(\epsilon_q - \epsilon_{q'})t - \cos(\epsilon_q + \epsilon_{q'})t]$  with  $\Gamma_{qq'} =$

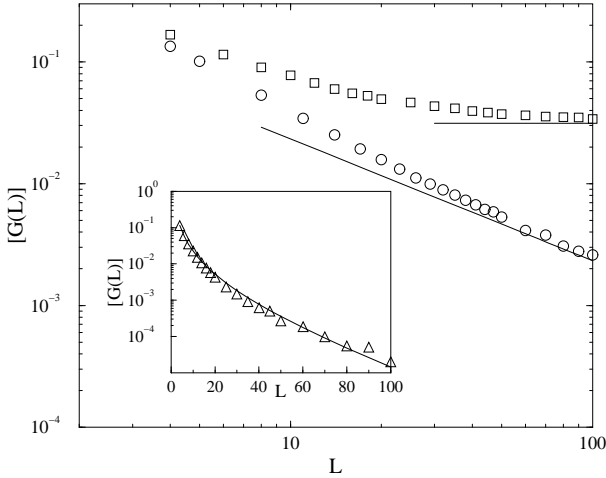


**Fig. 5.** Size dependence of the asymptotic value  $[G(L)]$  for  $h_o = h_c$  (circles),  $h_o = 0.8h_c$  (squares). Inset : Size dependence of the asymptotic value  $C_L^x(\infty)$  for  $h_o = 1.2h_c$  (triangles). The solid lines indicate the analytical predictions.

$\phi_q(1)\phi_{q'}(1)\psi_q(L)\psi_{q'}(L)$ . For  $t \gg 1$ , the arguments of the cosines are random phases and the  $F(L, t)$  contribution vanishes. In fact, since the bottom spectrum is behaving at the critical point as  $\epsilon_q \sim \exp(-\text{const.}L^{1/2})$  [13], the phases will be random for  $t > \epsilon^{-1} \sim \exp(\text{const.}L^{1/2})$ . The average correlator is thus asymptotically given by

$$[C_L^x(t \gg 1)] \simeq [G(L)]. \quad (26)$$

In the sum over all the modes, the dominant contribution comes from the lowest mode which is localized near the surface, the others being exponentially smaller. Thus, for large sizes one has

$$[G(L)] = \frac{1}{2} \sum_q [\phi_q^2(1)\psi_q^2(L)] \propto [\phi_1^2(1)\psi_1^2(L)]. \quad (27)$$

Physically, for a first excitation  $\epsilon_1$  vanishing faster than  $1/L$ ,  $\phi_1(1)$  and  $\psi_1(L)$  give the equilibrium magnetisation in the  $x$  direction at both boundaries [22,23]. One has

$$\langle \sigma_1^x \rangle = \phi_1(1) = \left( 1 + \sum_{i=1}^{L-1} \prod_{j=1}^i \left( \frac{h_j}{J_j} \right)^2 \right)^{-1/2}, \quad (28)$$

and a similar expression for  $\langle \sigma_L^x \rangle$  with  $h_j/J_j$  replaced by  $h_{L-j}/J_{L-j}$ . At the critical point, for a typical sample the fluctuations of the couplings generated along the chain lead to

$$\sum_i^{L-1} \prod_{j=1}^i \left( \frac{h_j}{J_j} \right)^2 \sim \exp(cL^{1/2}) \quad (29)$$

thanks to the central limit theorem, where  $c$  is a positive constant. So that the contribution to the average  $[G(L)]$  of a typical sample is of order  $\exp(-cL^{1/2})$ . Stronger contributions to the average  $[G(L)]$  come from rare samples

where the sum  $\sum_i^{L-1} \prod_{j=1}^i (h_j/J_j)^2$  is of order one. As noticed in several previous works [13,24,25] we can relate this problem to the surviving probability of a one-dimensional walker making  $L$  steps with an absorbing boundary at the origin. The quantity  $[G(L)]$  is related to the probability  $P_L(0 < y_i < y_L)$  that a walker starting near the origin, on the positive side, ends after  $L$  steps at a position  $y_L$  larger than all previous positions  $y_i$  without visiting negative sites. This is due to the fact that in  $[G(L)]$  it is the product of both right and left magnetisations that enter. For  $\delta = 0$ , that is at the critical point, the walker is unbiased and from the walker interpretation one has  $[G(L)] \sim 1/L$ . On the contrary for  $\delta > 0$  there is a drift proportional to  $\delta$  toward the absorbing boundary. In this case, contributions of order one are very rare and the average  $[G(L)]$ , proportional to the surviving probability, scales as  $L^{-3/2} \exp(-aL)$  with  $a > 0$  a constant [13]. This form fits very well the data as it could be seen in the inset of figure 5. For  $\delta < 0$ , that is in the ferromagnetic phase, the walker is drifted off the absorbing boundary and for  $L$  sufficiently large, the typical fluctuations of order  $L^{1/2}$  are not sufficient to make the walker cross the origin.  $[G(L)]$  is reaching a finite constant for  $L$  large enough. It is interesting to notice again here that it is the connected part of the average end-to-end non-equilibrium correlator  $[C_L^x(t)]$  that reaches a constant for  $t \gg 1$ . These three different regimes are summarized in figure 5. Same arguments can be applied to explain the similar behaviour of the average correlator  $[C_L^z(t)]$ .

## 4 Summary

We have studied numerically the non-equilibrium relaxation properties of the random Ising quantum chain by calculating the average transverse magnetisation and end-to-end correlation functions. Starting with a fully magnetised initial state, the random system relaxes toward a stationary state. The relaxation of the average transverse magnetisation, toward a constant value depending on the transverse field, is clearly not exponential due to the presence of too large oscillations, but most probably algebraic. For the same reasons it is hard to extract from the numerics the exact algebraic decay. This behaviour looks like the decay of the pure model without any disorder. Nevertheless, contrary to the pure case where quantum interference plays a central role, in the disordered system the averaging process over many samples is predominant.

The time-evolution of the end-to-end correlations, which gives some simple insight of the development of the spatial correlations in the quantum chain, is somehow more instructive. For times smaller than a threshold time  $\tau(L)$ , they vanish since both ends are not causally connected. After this limiting time, they start to grow up and for very long times they finally reach a constant value depending on the transverse field and on the system size. For the  $|x\rangle$  initial state, utilising a random walk argument, one can explain the scaling of this stationary size-dependent value. At the critical field, the main contribution to the average correlation comes from rare samples

that are strongly correlated due to large domains of strong bonds, giving a contribution of order one, while the contribution of a typical sample is exponentially small with the system size. So the average value is completely determined by the distribution of rare samples. This leads to a  $1/L$  scaling behaviour of the stationary value. In the ordered phase, the contribution of strongly correlated domains is very important and gives rise to a size-independent stationary value, as confirmed by the drifted walker analogy. On contrary, for a large transverse field, the walker is driven toward the absorbing boundary, as explained in the previous section, and the stationary value behaves as  $\exp(-cL)$ . In conclusion, contrary to the pure chain where after a sudden jump to a value  $L^{-a}$  at  $t = \tau(L)$ , the threshold time [9], the end-to-end correlation decreases toward zero with a stretched exponential like behaviour, in the disordered case the asymptotic behaviour is simpler. This discrepancy lies again in the fact that quantum interferences in the pure case are important while they play no significant role in the averaging process in the disordered situation. The stationary behaviour is just related to the statistical distribution of large strongly correlated domains.

Acknowledgements: Useful discussions with Christophe Chatelain are gratefully acknowledged.

## References

1. T. Niemeijer, *Physica* **36**, 377 (1967)
2. J. A. Tjion, *Phys. Rev. B* **2**, 2411 (1970)
3. R. H. Terwiel and P. Mazur, *Physica* **32**, 1813 (1966)
4. G. O. Berim, *Sov. Phys. JETP* **75**, 86 (1992)
5. T. Antal, Z. Rácz, A. Rákos and G. M. Schütz, *Phys. Rev. E* **59**, 4912 (1999)
6. G. M. Schütz and S. Trimper, *Europhys. Lett.* **47**, 164 (1999)
7. G. O. Berim, S. Berim and G. G. Cabrera, *Phys. Rev. B* **66**, 094401 (2002)
8. D. Karevski, *Eur. Phys. J. B* **27**, 147 (2002)
9. F. Iglói and H. Rieger, *Phys. Rev. Lett.* **85**, 3233 (2000)
10. S. K. Ma, C. Dasgupta and C. K. Hu, *Phys. Rev. Lett.* **43**, 1434 (1979)
11. D. S. Fisher, *Phys. Rev. Lett.* **69**, 534 (1992); *Phys. Rev. B* **51**, 6411 (1995)
12. A. P. Young and H. Rieger, *Phys. Rev. B* **53**, 8486 (1996)
13. F. Iglói and H. Rieger, *Phys. Rev. B* **57**, 11404 (1998)
14. F. Iglói and H. Rieger, *Phys. Rev. E* **58**, 4238 (1998)
15. F. Iglói, L. Turban and H. Rieger, *Phys. Rev. E* **59**, 1465 (1999)
16. R. B. Griffiths, *Phys. Rev. Lett.* **23**, 17 (1969)
17. B. McCoy, *Phys. Rev. Lett.* **23**, 383 (1969)
18. F. Iglói, R. Juhász and P. Lajkó, *Phys. Rev. Lett.* **86**, 1343 (2001)
19. F. Iglói, *Phys. Rev. B* **65**, 064416 (2002)
20. P. Jordan and E. Z. Wigner, *Z. Phys.* **47**, 631 (1928)
21. E. Lieb, T. Schultz and D. Mattis, *Ann. Phys. (N.Y.)* **16**, 407 (1961)
22. I. Peschel, *Phys. Rev. B* **30**, 6783 (1984)
23. D. Karevski, *J. Phys. A: Math. Gen.* **33**, L313 (2000)
24. F. Iglói, D. Karevski and H. Rieger, *Eur. Phys. J. B* **5**, 613 (1998)
25. D. Karevski, R. Juhász, L. Turban and F. Iglói, *Phys. Rev. B* **60**, 4195 (1999)